

Dendritic Arenethiol-Based Capping Strategy for Engineering Size and Surface Reactivity of Gold Nanoparticles

Hong Yan,^{†,§} Christina Wong,[‡] Anthony R. Chianese,[‡] Jin Luo,[†] Lingyan Wang,[†] Jun Yin,[†] and Chuan-Jian Zhong^{*,†}

[†]Department of Chemistry, State University of New York at Binghamton, Binghamton, New York 13902, United States, and [‡]Chemistry Department, Colgate University, Hamilton, New York 13346, United States.

[§]Current address: Department of Chemistry, Hunan University, Changsha, Hunan, 410082, China.

Received July 16, 2010. Revised Manuscript Received September 13, 2010

The report describes a strategy for the synthesis of gold nanoparticles for which size and surface reactivity of the particles are controlled by the molecular sizes of dendritic arenethiols (DAT) as capping agents. This strategy exploits two important attributes of the DAT molecules: one involving the utilization of the umbrella-like structure with a single thiol as the anchorage handle and the other involving the rib with an expandable dendritic structure as a spacing-tunable cap. The synthesis of gold nanoparticles with controllable sizes below 10 nm has been demonstrated using different sizes of DAT in both one-phase and two-phase solutions. The unique structural properties of the dendritic arenethiol capping molecules not only enable the ability to control size growth of gold nanoparticles but also ready surface exchange reaction for surface derivatization and interparticle assembly. The viability of this strategy for the control of size and surface reactivity has been demonstrated by results from the structural and morphological characterizations of the nanoparticles and assemblies.

Introduction

In recent years, functionalized gold nanoparticles are attracting increasing interest due to the different applications such as optoelectronic nanodevices,¹ chemical sensors,² nanotechnology,³ and biological sciences.⁴ The two-phase method reported first by Brust and Schiffrin has been widely used for the synthesis of gold nanoparticles capped with alkanethiols and other thiols which involved using tetraoctylammonium bromide (TOABr) as phase transfer agent.⁵ The presence of TOABr in the resulting gold nanoparticles was also recognized, which may affect the properties of the nanoparticles. Kaifer and co-workers reported a single-phase (e.g., in dimethylsulfoxide, DMSO) procedure to synthesize the cyclodextrin-modified gold nanoparticles.⁶ Recently, a simple one-phase method which successfully produced and stabilized gold nanoparticles

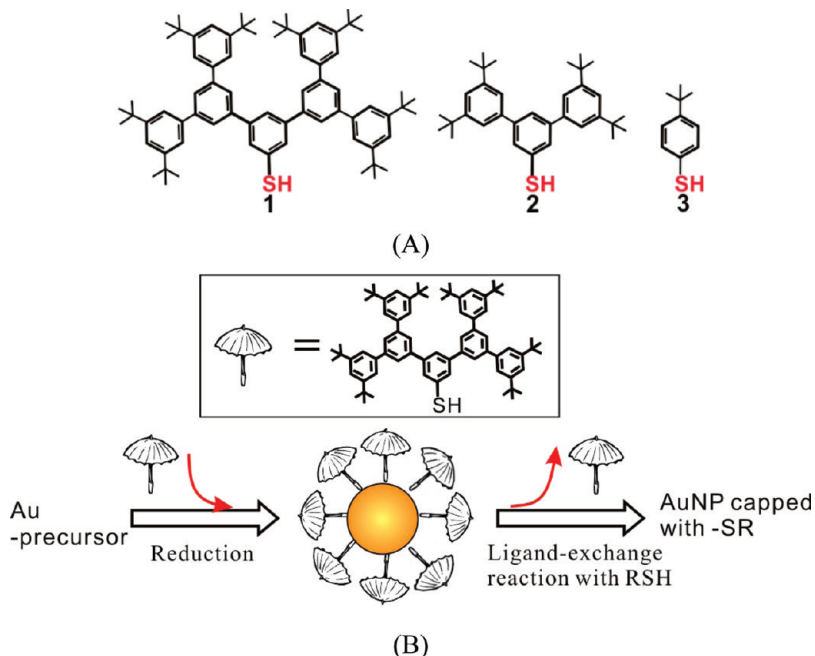
using porphyrin-based surface passivant ligand in *N*, *N*-dimethylformamide (DMF) was reported by Yutaka Hitomi.⁷ In these reports, the phase transfer agent was found to be unnecessary in the synthesis procedure. In these methods, the synthesis involved the reduction of Au^{3+} ions to gold atoms and nanoparticles by reducing agent NaBH_4 . The possible precipitation of the nanoparticle aggregation is detrimental to the control of the particle sizes. To prevent the particles from aggregating, one common approach involved the use of stabilizing agent that sticks to the nanoparticle surface.⁸ The stabilizing agent not only passivates the aggregation but also functionalizes the surface of the gold nanoparticles. The control of the size of the gold particles has often relied on controlling the functional groups,⁹ the concentration ratio of capping thiols to Au, or the lengths of alkyl chain in capping molecules.¹⁰ It is increasingly important to design molecular capping agents that can control both the size and the surface properties of gold nanoparticles.

The report describes a strategy of synthesis for the control of size and surface reactivity of gold nanoparticles using dendritic arenethiol (DAT) molecules of different sizes as capping agents. As illustrated by structures **1**, **2**,

- *To whom correspondence should be addressed. E-mail: cjzhong@binghamton.edu.
- (1) (a) Delden, R. A. v.; Wiel, M. K. J. t.; Pollard, M. M.; Vicario, J.; Koumura, N.; Feringa, B. L. *Nature* **2005**, 1337. (b) Kudernac, T.; Katsonis, N.; Browne, W. R.; Feringa, B. L. *J. Mater. Chem.* **2009**, 19, 7168.
(2) (a) Haes, A. J.; Duyne, R. P. V. *Anal. Bioanal. Chem.* **2004**, 379, 920. (b) Thomas, K. G.; Kamat, P. V. *Acc. Chem. Res.* **2003**, 36, 888. (c) Mirkin, C. A.; Letsinger, R. L.; Mucic, R. C.; Storhoff, J. J. *Nature* **1996**, 382, 607.
(3) (a) Shenhar, R.; Rotello, V. *Acc. Chem. Res.* **2003**, 36, 549. (b) Sastry, M.; Rao, M.; Ganesh, K. N. *Acc. Chem. Res.* **2002**, 35, 847.
(4) Aaron, J.; Travis, K.; Harrison, N.; Sokolov, K. *Nano Lett.* **2009**, 9, 3612.
(5) Brust, M.; Walker, M.; Bethell, D.; Schiffrin, D. J.; Whyman, R. *J. Chem. Soc., Chem. Commun.* **1994**, 801.
(6) (a) Liu, J.; Mendoza, S.; Roman, E.; Lynn, M. J.; Xu, R.; Kaifer, A. E. *J. Am. Chem. Soc.* **1999**, 121, 4304. (b) Liu, J.; Alvarez, J.; Kaifer, A. E. *Adv. Mater.* **2000**, 12, 1381.

- (7) Ohyama, J.; Hitomi, Y.; Higuchi, Y.; Shinagawa, M.; Mukai, H.; Kodera, M.; Teramura, K.; Shishido, T.; Tanaka, T. *Chem. Commun.* **2008**, 6300.
(8) (a) Liu, Y.; Yang, Y. W.; Chen, Y. *Chem. Commun.* **2005**, 4208. (b) Patel, G.; Menon, S. *Chem. Commun.* **2009**, 3563.
(9) Daniel, M.-C.; Astruc, D. *Chem. Rev.* **2004**, 104, 293.
(10) (a) Templeton, A. C.; Wueffling, W. P.; Murray, R. W. *Acc. Chem. Res.* **2000**, 33(1), 27. (b) Zhang, S.; Leem, G.; Lee, T. R. *Langmuir* **2009**, 25(24), 13855. (c) Hou, W.; Dasog, M.; Scott, R. W. J. *Langmuir* **2009**, 25, 2112.

Scheme 1. (A) Structures of the Dendritic Arenethiols: (1) 3,5-bis(3,5-bis(3,5-di-*t*-Butylphenyl)phenyl)benzenethiol, (2) 3,5-bis(3,5-di-*t*-butylphenyl)benzenethiol, and (3) *t*er-Butylbenzenethiol. (B) Illustration of the Exploitation of the Umbrella-Like DAT Molecules in the Utilization of the Structure with a Single Thiol as the Anchorage Handle and the Rib with an Expandable Dendritic Structure as a Spacing-Tunable Cap for Tuning the Nanoparticle Sizes and Surface Reactivities



and **3** in Scheme 1, two important attributes of the umbrella-like DAT molecules can be exploited. One involves the utilization of the umbrella-like structure with a single thiol as the anchorage handle, and the other exploits the rib with an expandable dendritic structure as a spacing-tunable cap. Findings from the characterization of the as-synthesized gold nanoparticles with controllable sizes below 10 nm and their surface reactivities will be discussed, focusing on understanding the viability of the DAT-based molecular tuning of size and surface reactivity.

Experimental Section

Chemicals. Hydrogen tetrachloroaurate (HAuCl_4 , 99%), tetraoctylammonium bromide (TOA^+Br^- , 99%), 11-mercaptopoundecanoic acid (MUA, 97%), decanethiol (DT, 96%), and sodium borohydride (NaBH_4 , 99%) were purchased from Aldrich and used as received. *t*er-Butylbenzenethiol ($\text{C}_{10}\text{H}_{14}\text{S}$, 98%) was purchased from Sigma-Aldrich and purified by thin layer chromatography before use. Other chemicals were purchased from Aldrich and used as received. Water was purified with a Millipore Milli-Q water system.

Synthesis of Dendritic Arenethiols (DAT). 3,5-di-*t*-Butylbeneneboronic acid¹¹ and 3,5-bis(3,5-di-*t*-butylphenyl)beneneboronic acid¹² were synthesized as previously described. All other materials were commercially available and were used as received, unless otherwise noted. Solvents were purified by sparging with argon and passing through columns of activated alumina, using a MBraun Solvent Purification System. Synthesis was performed using dried and degassed solvents under inert atmosphere, using standard Schlenk techniques. NMR spectra were recorded at room temperature on a Bruker spectrometer operating at

400 MHz (¹H NMR) and 100 MHz (¹³C NMR and referenced to tetramethylsilane (δ in parts per million and J in Hz)). Mass spectrometry was performed by the Mass Spectrometry Laboratory at the University of Illinois at Urbana-Champaign.

Protected 3,5-Dibromobenzenethiol 4. In a modification of a procedure reported by Itoh and Mase,¹³ 1,3,5-tribromobenzene (2.00 g, 6.35 mmol), $\text{Pd}(\text{dibenzylideneacetone})_3$ (93 mg, 0.106 mmol), and bis(2-diphenylphosphinophenyl)ether (DPEPhos, 114 mg, 0.212 mmol) were added to a flame-dried Schlenk flask. The flask was evacuated and backfilled with argon three times. Toluene (30 mL) and diisopropylethylamine (2.22 mL, 12.7 mmol) were added, followed by mercaptopropionic acid 2-ethylhexyl ester (0.76 mL, 4.24 mmol). The solution was stirred at 100 °C for 16 h and then was allowed to cool to room temperature. The mixture was filtered through a short plug of silica gel and eluted with 100 mL of diethyl ether. The volatiles were removed, and the residue was purified by flash chromatography on silica gel and eluted with 2% ethyl acetate in hexanes. The product was isolated as a yellow liquid. Yield: 1.63 g, 85%. ¹H NMR (CDCl_3 , 400 MHz): 7.50 (t, 1H, $^4J_{\text{HH}} = 1.8$ Hz); 7.40 (d, 2H, $^4J_{\text{HH}} = 1.8$ Hz); 4.05 (m, 2H); 3.20 (t, 2H, $^3J_{\text{HH}} = 7.2$ Hz); 2.67 (t, 2H, $^3J_{\text{HH}} = 7.2$ Hz); 1.58 (m, 1H); 1.24–1.40 (m, 8H); 0.92 (t, 6H, $^3J_{\text{HH}} = 7.5$ Hz). ¹³C NMR (CDCl_3 , 100 MHz): 171.4, 140.0, 131.7, 130.0, 123.2, 67.4, 38.7, 34.0, 30.4, 28.9, 28.6, 23.8, 23.0, 14.1, 11.0. HRMS (EI+): calcd for $\text{C}_{17}\text{H}_{24}\text{O}_2\text{Br}_2\text{S}$, 449.9864; found, 449.9862.

Protected First-Generation Thiol 5. According to Buchwald's optimized procedure for Suzuki couplings,¹⁴ protected thiol **4** (193 mg, 0.43 mmol), 3,5-di-*t*-butylbeneneboronic acid (300 mg, 1.28 mmol), $\text{Pd}(\text{OAc})_2$ (2.2 mg, 10 mmol), 2-dicyclohexylphosphino-2',6'-dimethoxy-1,1'-biphenyl (SPhos, 8.2 mg, 20 mmol), and K_3PO_4 (365 mg, 1.72 mmol) were added to a flame-dried Schlenk flask. The flask was evacuated and backfilled with

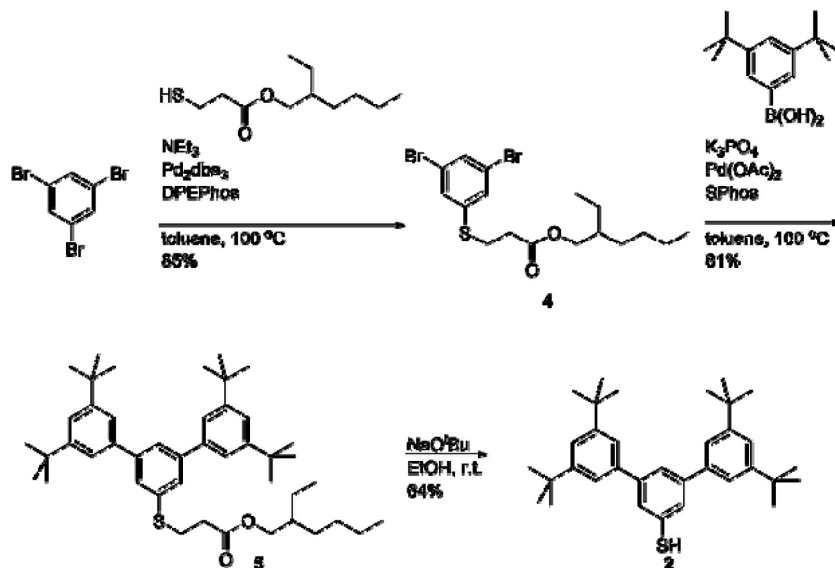
(11) Nomura, N.; Ishii, R.; Yamamoto, Y.; Kondo, T. *Chem.-Eur. J.* **2007**, *13*, 4433.

(12) Chianese, A. R.; Mo, A.; Datta, D. *Organometallics* **2009**, *28*, 465.

(13) Itoh, T.; Mase, T. *J. Org. Chem.* **2006**, *71*, 2203.

(14) Walker, S. D.; Barder, T. E.; Martinelli, J. R.; Buchwald, S. L. *Angew. Chem., Int. Ed.* **2004**, *43*, 1871.

Scheme 2. Schematic Illustration for the Synthesis of 2



argon three times. Toluene (10 mL) was added, and the mixture was stirred at 100 °C for 16 h. The mixture was then cooled to room temperature, diluted with 50 mL diethyl ether, filtered through a plug of silica gel, and eluted with an additional 50 mL of diethyl ether. The volatiles were removed, and the residue was purified by flash chromatography on silica gel and eluted with 1% ethyl acetate in hexanes. Yield: 235 mg, 81%. ¹H NMR ($CDCl_3$, 400 MHz): 7.63 (t, 1H, $^4J_{HH}$ = 1.4 Hz); 7.57 (d, 2H, $^4J_{HH}$ = 1.4 Hz); 7.52 (t, 2H, $^4J_{HH}$ = 1.7 Hz); 7.47 (d, 4H, $^4J_{HH}$ = 1.7 Hz); 4.05 (m, 2H); 3.32 (t, 2H, $^3J_{HH}$ = 7.2 Hz); 2.76 (t, 2H, $^3J_{HH}$ = 7.2 Hz); 1.58 (m, 1H); 1.24–1.40 (m, 44H); 0.90 (t, 6H, $^3J_{HH}$ = 7.5 Hz). ¹³C NMR ($CDCl_3$, 100 MHz): 171.9, 151.3, 143.9, 140.3, 135.9, 127.7, 125.6, 121.9, 121.9, 67.2, 38.7, 35.0, 34.7, 31.5, 30.4, 29.3, 28.9, 23.8, 23.0, 14.1, 11.0. Note: The overlap of the aromatic carbons ortho and para to the thiol substitution at δ 121.9 was confirmed by HMQC. HRMS (EI+): calcd for $C_{43}H_{66}O_2S$, 670.4784; found, 670.4786.

First-Generation Thiol 2 (Scheme 2). In a modification of a procedure reported by Itoh and Mase,¹³ the protected thiol **5** (183 mg, 0.273 mmol) was added to a small vial, along with 5 mL of absolute ethanol and NaO^tBu (450 mg, 4.9 mmol). The solution was stirred and monitored for completion by thin-layer chromatography (TLC). After 30 min, the reaction was complete and the solution was transferred to a separatory funnel along with 20 mL of aqueous ammonium chloride and 20 mL of dichloromethane. The organic layer was collected, and the aqueous layer was extracted with an additional 20 mL of dichloromethane. The organic fractions were combined, dried over $MgSO_4$, filtered, and concentrated. The residue was purified by flash chromatography on silica gel and eluted with 1% ethyl acetate in hexanes. Yield: 93 mg, 70%. ¹H NMR ($CDCl_3$, 400 MHz): 7.57 (t, 1H, $^4J_{HH}$ = 1.4 Hz); 7.49 (t, 2H, $^4J_{HH}$ = 1.8 Hz); 7.46 (d, 2H, $^4J_{HH}$ = 1.4 Hz); 7.44 (d, 4H, $^4J_{HH}$ = 1.8 Hz); 3.64 (s, 1H, SH), 1.40 (s, 36H). ¹³C NMR ($CDCl_3$, 100 MHz): 151.3, 144.0, 140.1, 131.2, 127.0, 124.6, 121.9, 121.8, 35.0, 31.5. HRMS (EI+): calcd for $C_{34}H_{46}S$, 486.3320; found, 486.3322.

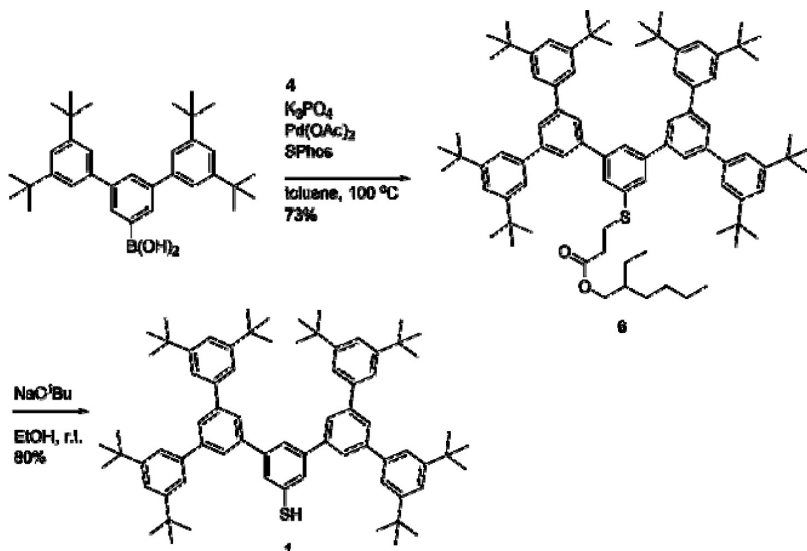
Protected Second-Generation Thiol 6. According to Buchwald's optimized procedure for Suzuki couplings, protected thiol **4** (60 mg, 0.133 mmol), 3,5-bis-(3,5-di-*t*-butylphenyl)beneneboronic acid (200 mg, 0.401 mmol), $Pd(OAc)_2$ (2.0 mg, 9 mmol), 2-dicyclohexylphosphino-2',6'-dimethoxy-1,1'-biphenyl (SPhos, 7.2 mg, 18 mmol), and K_3PO_4 (169 mg, 0.798 mmol) were added to a flame-dried Schenck flask. The flask was evacuated and back-filled with argon three times. Toluene (10 mL) was added, and the

mixture was stirred at 100 °C for 16 h. The mixture was then cooled to room temperature, diluted with 50 mL of diethyl ether, filtered through a plug of silica gel, and eluted with an additional 50 mL of diethyl ether. The volatiles were removed, and the residue was purified by flash chromatography on silica gel and eluted with 1% ethyl acetate in hexanes. Yield: 140 mg, 88%. ¹H NMR ($CDCl_3$, 400 MHz): 7.82 (t, 1H, $^4J_{HH}$ = 1.6 Hz); 7.79 (t, 2H, $^4J_{HH}$ = 1.7 Hz); 7.77 (d, 4H, $^4J_{HH}$ = 1.7 Hz); 7.71 (d, 2H, $^4J_{HH}$ = 1.6 Hz); 7.51 (s, 12H); 4.01 (m, 2H); 3.32 (t, 2H, $^3J_{HH}$ = 7.2 Hz); 2.76 (t, 2H, $^3J_{HH}$ = 7.2 Hz); 1.58 (m, 1H); 1.24–1.40 (m, 80H); 0.90 (t, 6H, $^3J_{HH}$ = 7.5 Hz). ¹³C NMR ($CDCl_3$, 100 MHz): 171.7, 151.3, 144.0, 143.1, 141.5, 140.8, 136.9, 127.5, 126.7, 125.6, 125.2, 122.0, 121.8, 67.3, 38.7, 35.0, 34.5, 31.6, 30.3, 28.93, 28.87, 23.7, 22.9, 14.0, 10.9. HRMS (ESI+): calcd for $C_{85}H_{114}NaO_2S$ ($M + Na$), 1221.8437; found, 1221.8431.

Second-Generation Thiol 1 (Scheme 3). In a modification of a procedure reported by Itoh and Mase, the protected thiol **4** (90 mg, 0.075 mmol) was added to a small vial, along with 2 mL of absolute ethanol and NaO^tBu (112 mg, 1.1 mmol). The solution was stirred and monitored for completion by TLC. After 60 min, the reaction was complete and the solution was transferred to a separatory funnel along with 10 mL of aqueous ammonium chloride and 10 mL of dichloromethane. The organic layer was collected, and the aqueous layer was extracted with an additional 10 mL of dichloromethane. The organic fractions were combined, dried over $MgSO_4$, filtered, and concentrated. The residue was purified by flash chromatography on silica gel and eluted with 1% ethyl acetate in hexanes. The product retained a small amount of hexane, even upon prolonged evaporation, and a small amount of hydrocarbon grease was visible by NMR after purification. Yield: 56 mg, 73%. ¹H NMR ($CDCl_3$, 400 MHz): 7.78 (t, 2H, $^4J_{HH}$ = 1.6 Hz); 7.77 (t, 1H, $^4J_{HH}$ = 1.5 Hz); 7.75 (d, 4H, $^4J_{HH}$ = 1.6 Hz); 7.64 (d, 2H, $^4J_{HH}$ = 1.5 Hz); 7.50 (t, 4H, $^4J_{HH}$ = 1.8 Hz); 7.48 (d, 8H, $^4J_{HH}$ = 1.8 Hz); 3.66 (s, 1H, SH), 1.40 (s, 72H). ¹³C NMR ($CDCl_3$, 100 MHz): 151.3, 144.0, 143.2, 141.3, 140.8, 132.3, 127.2, 126.7, 125.4, 124.3, 122.0, 121.8, 35.0, 31.6. The molecular ion was not observed by ESI-MS or MALDI-MS, under a variety of ionization conditions.

Synthesis of DAT-Capped Gold Nanoparticles. Two methods, a two-phase method and a single-phase method, were used to synthesize the dendritic arenethiol-modified gold nanoparticles.

Scheme 3. Schematic Illustration for the Synthesis of 1



Two-Phase Method. The two-phase method employed standard literature procedures.^{5,10} A typical synthesis is as follows: 30 mL of an aqueous solution of HAuCl₄·3H₂O (0.1 mmol) was stirred with a solution of tetraoctylammonium bromide (TOABr, 1 mmol) in 40 mL of toluene until all the Au³⁺ was transferred to the organic layer and the water layer became colorless. Dendritic arenethiol (0.1 mmol) was then added to the organic phase. After stirring for several minutes, 10 mL of a freshly prepared NaBH₄ (40 mg, 0.1 mmol) solution was added over 20 min, and the solution was stirred for the next 4 h. Excess thiol and TOABr impurities were removed by washing with ethanol.

Single-Phase Method. The single-phase method was used to synthesize the dendritic arenethiol-protected gold nanoparticles, which is similar to the methods reported by others.^{6,7} A typical synthesis is as follows: 20 mL of C₂H₅OH solution of HAuCl₄·3H₂O (0.1 mmol) was added into 20 mL of chloroform solution of dendritic arenethiol (0.1 mmol). Then, NaBH₄ (1 mmol, solid state) was added directly. The solution turned from bright orange to dark purple gradually with the addition of NaBH₄, indicating the formation of gold nanoparticles. After addition, the mixture was stirred for 4 h. The organic layer was evaporated in vacuo; excess dendritic arenethiol and NaBH₄ impurities were removed by washing with ethanol and water. After the residue was dispersed into water by sonicating, the water phase was extracted with ethyl acetate until the water phase was colorless. The extract was dried over MgSO₄, and filtered. The solvent was evaporated in vacuo, and the residue was dissolved in toluene.

Instrumentation and Measurements. Transmission electron microscopy (TEM) was performed on a Hitachi H-7000 electron microscope (100 kV). TEM samples were taken from the solutions of dendritic arenethiol-modified gold nanoparticles. Typically, the TEM samples were prepared by taking a solution sample and casting it onto a carbon-coated copper grid sample holder followed by evaporation in air at room temperature. UV-vis spectra were collected using an HP 8453 spectrophotometer. Spectra were collected over the range of 200–1100 nm, and the baseline of each spectrum was corrected by subtracting a spectrum of the corresponding solvent. All samples were placed in a quartz cuvette having a 1.0 cm optical path length. Fourier transform infrared (FTIR) spectra were acquired with a Nicolet 760 ESP FTIR spectrometer that was purged with boil-off from liquid N₂. Surface enhanced Raman spectroscopy (SERS)

spectra were recorded using the Advantage 200A Raman instrument (DeltaNu). The instrument collects data over 200–3400 cm⁻¹. The Raman spectra of nanoparticles in the solid state were collected by placing an aliquot of the solution on the gold surface and allowing the solvent to evaporate prior to data collection. All glassware used in the preparation and storage of the Au nanoparticles (NPs) was treated with aqua regia and rinsed with water.

Molecular modeling and theoretical Raman spectra for dendritic arenethiols were calculated using Gaussian 3.0. All the semiempirical calculations were performed on an Opt+Freq computational package implemented in Gaussian 3.0 software. The computational procedure included geometry optimization at the Restricted Hartree-Fock 3-21G level of theory.

Results and Discussion

Composition and Morphology. The gold nanoparticles capped by DAT (AuNP-DAT) synthesized by the two-phase and single-phase methods were examined. The nanoparticles with different DAT capping molecules 1, 2, and 3 are represented by Au@1, Au@2, and Au@3, respectively. Note that the numbers 1, 2, and 3 are simply used for abbreviating the DAT molecules and are not referring to generation bombers as used in describing the increase of size in dendrimers or dendrons.

Au@1, Au@2, and Au@3 Synthesized by Two-Phase Method. Figure 1 shows a representative set of the TEM images of gold nanoparticles synthesized by the two-phase method. The average particle sizes were found to be 4.2 nm (Au@1), 3.9 nm (Au@2), and 2.8 nm (Au@3), respectively, showing an order of decreasing particle size with a decrease in the molecular size of DAT. The presence of clustered or aggregated features is evident for these as-synthesized nanoparticles. This finding is in contrast to the synthesis of gold nanoparticles in the presence of only TOABr, which was shown to produce particles sizes of 5 to 6 nm⁵, corresponding to TOABr-capped gold nanoparticles.

Figure 2 shows a representative set of UV-vis spectra for the DAT-capped gold nanoparticles. The surface

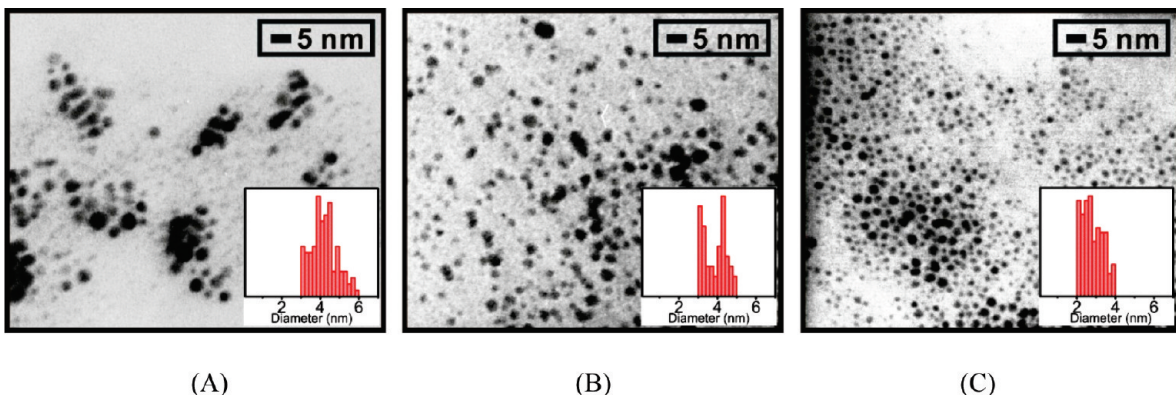


Figure 1. TEM micrographs for two-phase method synthesized gold nanoparticles (A) Au@1 (4.2 ± 0.7 nm); (B) Au@2 (3.9 ± 0.6 nm); (C) Au@3 (2.8 ± 0.5 nm).

plasmon bands were found around 520 nm. The band position is characteristic of the gold nanoparticles in this size range.

Because of the use of TOABr as phase transfer agent in the two-phase synthesis, it is difficult to completely remove the excess TOABr from the as-synthesized DAT-capped gold nanoparticles even by extensive washing. The presence of traces of TOABr in the nanoparticle was believed to be partially responsible for the highly clustered or aggregated features observed in Figure 1. The formation of such features involves van der Waals interactions between alkyl chains of TOABr and DAT molecules in the capping monolayer structures.

Au@1, Au@2, and Au@3 Synthesized by Single-Phase Method.

In the case of the one-pot reduction of HAuCl₄ in a single-phase solution (EtOH/CHCl₃), the only capping agents were DAT molecules because the reaction was carried out in the absence of TOABr. CHCl₃/CH₃OH was used as a single-phase solvent because this solvent can be easily removed after the synthesis. Note that the single-phase procedure was used to synthesize gold nanoparticles previously^{6,7} where DMSO or DMF was used as solvent. Such solvent is difficult to be removed after the synthesis. Unlike this previous method that used NaBH₄ dissolved in aqueous solution as reducing agent, we added the reducing agent NaBH₄ in solid state. This approach was found to be effective in preventing the gold nanoparticles from the propensity of precipitation. In this case, gold nanoparticles were produced slowly by reaction with the reducing agent NaBH₄ in solid state, as shown by the slow color change, in contrast to the fast color change in the previous method.⁸

Figure 3 shows a set of TEM images of DAT-capped gold nanoparticles synthesized by the single-phase method. In this single-phase synthesis solution, an identical molar ratio of gold to ligand (1:1) was used for all three DAT molecules. In comparison with the clustered features for the two-phase synthesized nanoparticles, the nanoparticles were found to be well separated. This was partly attributed to a better encapsulation of DAT molecules in the absence of TOABr in the synthesis solution. Importantly, the size of the DAT-capped gold nanoparticles was again found to exhibit the order of Au@1

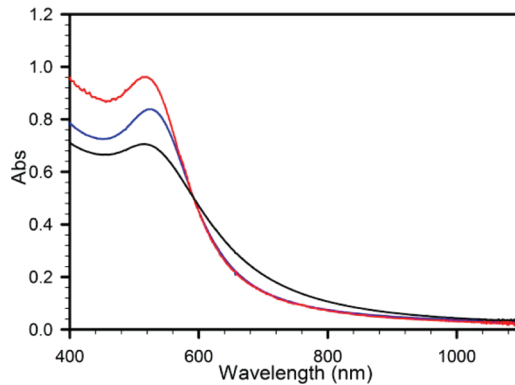


Figure 2. UV-vis spectra comparing the surface plasmon (SP) band characteristics of Au@1 (red), Au@2 (blue), and Au@3 (black) synthesized by the two-phase method. The particles were washed with ethanol.

(5.8 ± 0.8 nm) > Au@2 (4.9 ± 0.6 nm) > Au@3 (2.9 ± 0.3 nm). This trend, in agreement with the trend observed for the two-phase synthesis, demonstrates clearly that the particle size is controlled by the molecular size of DAT.

The surface plasmon band of Au@1, Au@2, and Au@3 were observed at 525, 520, and 515 nm, respectively (Figure 4). The intensity and position of the surface plasmon bands are consistent with the observed trend for the particle size determined from TEM data and the color of Au@1, Au@2, Au@3 nanoparticles.

It is evident that both two-phase and single-phase methods produced gold nanoparticles with sizes being dependent on the molecular size of the capping DAT. Although gold nanoparticles could be formed by NaBH₄ reduction of HAuCl₄ in CHCl₃/CH₃OH without DAT molecules, the resultant gold nanoparticles were unstable and easily precipitated as aggregates. In contrast, the gold nanoparticles Au@1, Au@2, and Au@3 were found to be very stable, as evidenced by lack of any changes in surface plasmon band and TEM size over weeks. This observation serves as an important piece of evidence supporting the effective capping of gold nanoparticles by dendritic arenethiol molecules. Additional experimental results (see Supporting Information, Figure S1) have also demonstrated that repetitive solvent washing or aging of the DAT-capped Au nanoparticles did not lead to any significant change in particle sizes or surface plasmon resonance

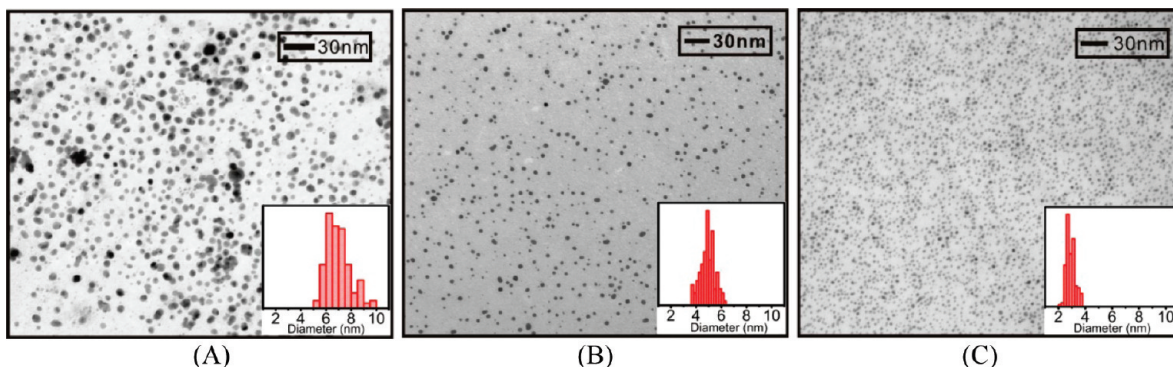


Figure 3. TEM images of Au@1 (A), Au@2 (B), and Au@3 (C) (synthesized by single-phase method) with histograms of particle size (inset: Au@1 (5.8 ± 0.8 nm); Au@2 (4.9 ± 0.6 nm); Au@3 (2.9 ± 0.3 nm)). The initial molar ratio of ligand and Au^{3+} is 1:1 for all cases.

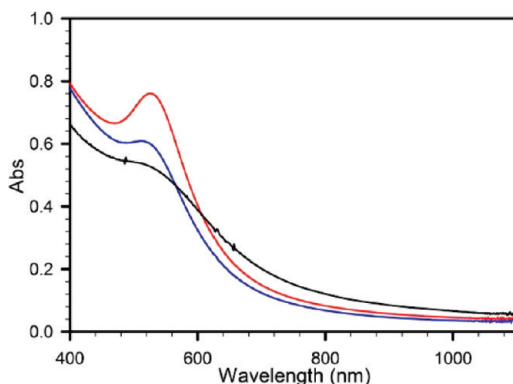


Figure 4. UV-vis spectra of Au@1 (red), Au@2 (blue), and Au@3 (black) (synthesized by single-phase method) in toluene after washing the as-synthesized particles with water.

band of the nanoparticles, demonstrating the stability of the particles as a result of the surface encapsulation by the dendritic arenethiol molecules.

The encapsulation of the gold nanoparticles by DAT molecules was further supported by spectroscopic characterizations. Figure 5 shows a representative set of Raman spectra for DAT-capped Au nanoparticles deposited on gold thin film substrates which is known to produce a SERS effect.¹⁵ The dendritic arenethiols are π -conjugated structures which consist of a single C–C bond connected to a benzene ring. Such structures in solid state showed the stretch vibration of the benzene ring at about 1600 cm^{-1} . In comparison, a peak was detected at similar position for the dendritic arenethiol-capped gold nanoparticles. The observation of this diagnostic stretching vibration of the benzene ring at about 1600 cm^{-1} indicates that the dendritic arenethiols are present in the capping structure of the as-synthesized gold nanoparticles. The Raman spectra of dendritic arenethiols in the solid state were compared with the theoretically predicted Raman spectra (see Supporting Information). The predicted spectra (calculated using Gaussian 3.0) and the experimental spectra are in general agreement in terms of the peak features, except the wavenumbers of some peaks in the experimental spectra are lower than theoretically predicted ones, which is

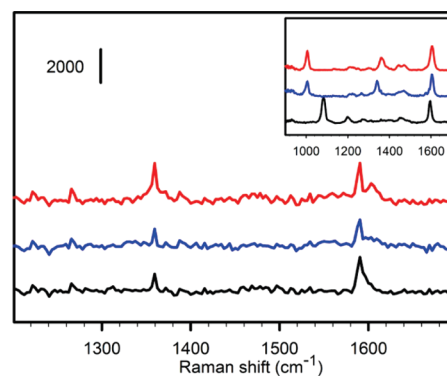


Figure 5. Raman spectra for DAT-capped Au nanoparticles of Au@1 (red), Au@2 (blue), and Au@3 (black) (synthesized by single-phase method) deposited on gold thin film substrates. Inset: Raman spectra for powder samples of DAT molecules: **1** (red), **2** (blue), and blank (black).

due to the fact that the partially coplanar nature of the benzene rings in DAT is not considered in Gaussian 3.0.

To assess the surface packing density of DAT capping molecules on the nanoparticles, the molecular geometry and size were considered based on molecular modeling. Table 1 shows the detailed molecular shape and structure for the DAT molecules. The dendritic arenethiols **1** and **2** consist of benzene rings connected through single C–C bonds. Due to the slight twist between the connected benzene rings, the angle between two adjacent benzene rings is found to be about 28.7 degrees (from Gaussian 3.0 calculation). The structures are also consistent with models based on crystal structures of metal complexes with dendritic side groups which showed a ~ 30 degree angle between the adjacent rings.

On the basis of the 3D molecular modeling and TEM-determined size of Au@1, Au@2, and Au@3, the approximate number of dendritic arenethiols (**1**, **2**, and **3**) in a densely packed monolayer assembly on the surface of the nanoparticle was estimated. Table 2 shows the predicted number of capping molecules on gold particle surfaces in two types of dense packing. (One involves a densely packed monolayer assembly, assuming a 3D molecular shape with a $L \times W \times H$ dimensions, on the surface of the nanoparticle (A_{\square}), and the other involves a densely packed monolayer assembly, assuming a spherical molecule with the long-dimension length as a diameter (d), on the surface of the

(15) Yan, H.; Lim, S. I.; Zhang, Y.; Chen, Q.; Mott, D.; Wu, W.; An, D. L.; Zhong, C. J. *Chem. Commun.* **2010**, 2218.

Table 1. Structural Comparison of Dendritic Arenethiols, 1, 2, and 3, Based on 3D Molecular Modeling

ligand	Long-side view	Short-side view	Top view	Size (nm) (L × W × H)
1				2.0×1.5×1.3
2				1.5×0.8×0.9
3				0.4×0.4×0.8

Table 2. Estimated Number of Ligands Per Particle and the Ligand-to-AuNP Ratios for DAT-Capped Gold Nanoparticles^a

ligand	AuNP size (nm)	type*	molecular geometry (L × W × H) for A_{\square} or diameter (d) for A_O	# of ligands per NP	L/AuNP ratio theor.	L/AuNP ratio wxptl.
1	6.0	A_{\square}	2.0 × 1.5 × 1.3	38	34:1	670:1
		A_O	2.5	29		
2	5.0	A_{\square}	1.5 × 0.8 × 0.9	65	50:1	380:1
		A_O	1.7	35		
3	3.0	A_{\square}	0.4 × 0.4 × 0.8	176	145:1	82:1
		A_O	0.6	113		

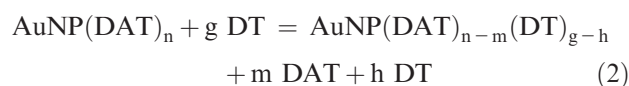
^a Note: Calculations were based on a densely packed monolayer assembly of the molecules on gold nanoparticle surface. A_{\square} represents a densely-packed monolayer assembly, assuming a 3D molecular shape with a $L \times W \times H$ dimensions, on the surface of the nanoparticle; A_O presents a densely-packed monolayer assembly, assuming a spherical molecule with the long-dimension length as a diameter (d), on the surface of the nanoparticle.

nanoparticle (A_O). The theoretical molar ratio between ligands and gold atoms is according to 3D molecular modeling and gold nanoparticle size. The experimental molar ratios between ligands and gold atoms were all 1:1 in the synthesis. In comparison with the theoretical values in terms of the number of ligands per NP, there is an excess amount of capping molecules. Note that for **3**, the experimental ratio of L/AuNP was somewhat less than the theoretical ratio. Additional experiments with increased ratios for L/AuNP for the case of **3**, e.g., L/AuNP = 400:1, the as-synthesized particles, did not show any significant changes in size and optical properties.

Surface Reactivity in the DAT Capping Monolayer of AuNP–DAT. Displacement of DAT in the Capping Monolayer by Free Thiols in Solution via Place-Exchange Reaction. To understand the viability of exploiting the umbrella-like structure with a single thiol handle and a spacing-tunable rib for tuning surface reactivity, the surface place exchange reaction of the DAT on the particle surface with alkanethiols in solution was investigated. The place-exchange reaction was pioneered by the

Murray group, which involves the replacement of one type of thiols (original capping molecules) on the gold nanoparticle surface by another type of thiols (free thiols from the solution).¹⁶ In this reaction, the product compositions were determined by ¹H NMR spectroscopy. Generally, a low feed ratio of the free-thiol vs the capping-thiol yields a low ratio of the two components on the nanoparticle surface, which can be explained by the exchange equilibrium. There are constraints on the amount of ω -substituted alkanethiol exchanged onto the capping monolayer of the nanoparticle surfaces presumably due to steric crowding in the monolayer's skin.¹⁶

In our work, the basic concept involves replacement of the DAT molecules by another type of alkanethiols (e.g., DT, MUA) which have a stronger binding ability to gold surface than DAT because of a stronger chain–chain cohesive energy in the capping monolayer. The exchange–replacement could be as high as 100%, as illustrated in eq 1, or partial, as illustrated in eq 2:



(16) (a) Hostetler, M. J.; Green, S. J.; Stokes, J. J.; Murray, R. W. *J. Am. Chem. Soc.* **1996**, *118*, 4212. (b) Wang, G.; Guo, R.; Kalyuzhny, G.; Choi, J.; Murray, R. W. *J. Phys. Chem. B* **2006**, *110*, 20282. (c) Song, Y.; Harper, A. S.; Murray, R. W. *Langmuir* **2005**, *21*, 5492.

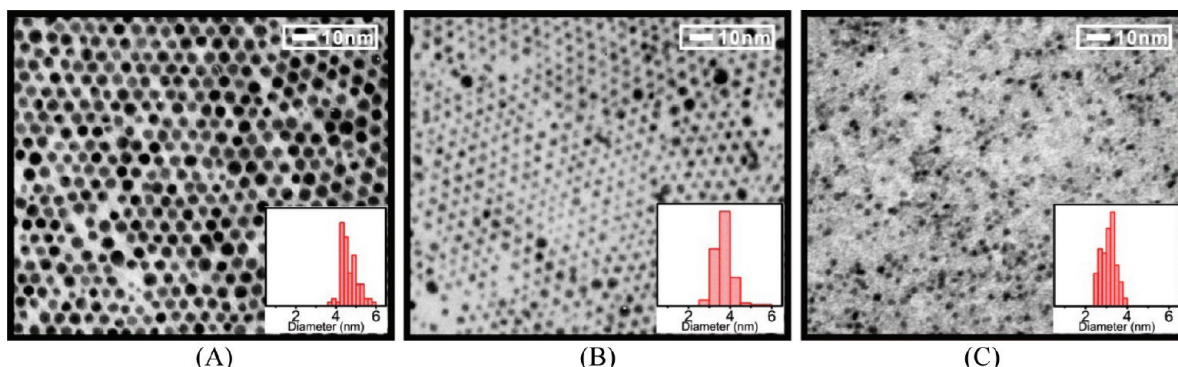


Figure 6. TEM micrographs and size distributions for DAT-capped Au nanoparticles (synthesized by two-phase method) after ligand exchange with decanethiols. (A) Au@1, 4.7 ± 0.5 nm; (B) Au@2, 3.7 ± 0.4 nm; (C) Au@3, 3.1 ± 0.3 nm.

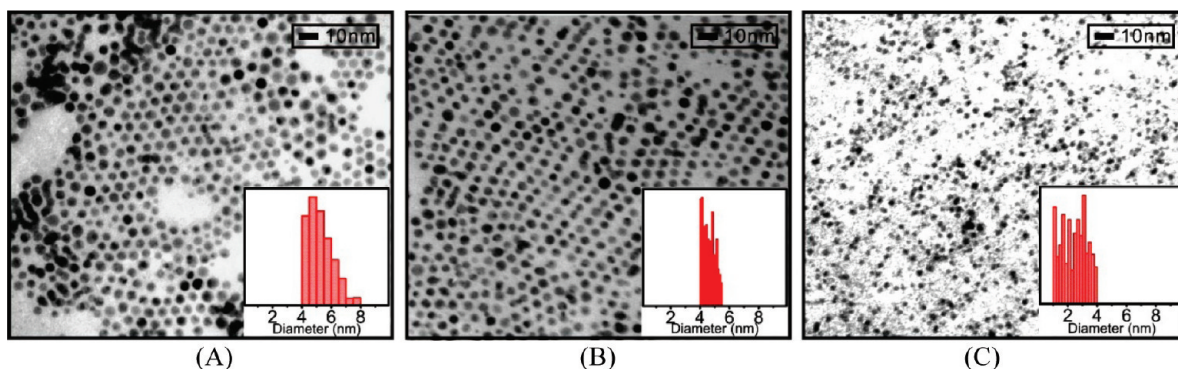


Figure 7. TEM micrographs of (A) Au@1, 5.3 ± 0.8 nm; (B) Au@2, 4.6 ± 0.4 nm; (C) Au@3, 2.4 ± 0.9 nm (synthesized by single-phase method) after ligand exchange with decanethiols. The measured interparticle edge-to-edge distance: Au@1 (1.8 ± 0.4 nm); Au@2 (1.9 ± 0.3 nm).

Figure 6 shows a typical set of TEM images for the nanoparticles after the exchange reaction of the two-phase synthesized Au@DAT particles (7.7×10^{19} particles/mL) in a solution containing DT (71 mM). It is evident the particles are all individually isolated and form ordered domains, in sharp contrast to the highly clustered or aggregated features for the particles before the exchange reaction. The particle size remained basically unchanged. For example, the two-phase synthesized gold nanoparticles showed 4.2 ± 0.7 nm for Au@1, 3.9 ± 0.6 nm for Au@2, and 2.8 ± 0.5 nm for Au@3. After exchange reaction with DT, the obtained sizes were 4.7 ± 0.5 nm for Au@1, 3.7 ± 0.4 nm for Au@2, and 3.1 ± 0.3 nm for Au@3. This finding demonstrates a very effective replacement of the DATs on particles by DTs from the solution, forming DT-capped Au nanoparticles.

A similar effectiveness of ligand exchange was also observed for the single-phase synthesized AuNP-DAT (Figure 7). After exchange reaction for Au@1 (A) and Au@2 (B), the particles are better individually isolated and form better-ordered domains in comparison with those before the exchange reaction. For Au@3, there does not appear to be a significant change after the exchange reaction. The measured interparticle edge-to-edge distance, 1.8 and 1.9 nm, for DT-exchanged Au@1 (A) and Au@2 (B) seems to be quite close to the distance expected based interdigititation of DT molecules capped on the nanoparticles. Insignificant changes in particle sizes were observed after the exchange reaction (e.g., 5.8 ± 0.8 nm

(Au@1), 4.9 ± 0.6 nm (Au@2), and 2.9 ± 0.3 nm (Au@3) for particles before exchange reaction; and 5.3 ± 0.8 nm (Au@1), 4.6 ± 0.4 nm (Au@2), and 2.4 ± 0.9 nm (Au@3) for particles after exchange reaction).

The replacement of DAT by DT was further examined by FTIR characterization of the samples. Figure 8 shows a representative set of FTIR spectra for the single-phase synthesized AuNP-DAT before and after exchange reaction with DT. The FTIR spectra for the DAT molecule and the as-synthesized DT-capped gold nanoparticles (2 nm) are also included for comparison. Before exchanging with DT, the FTIR spectra in the high frequency (C-H stretching) and low frequency regions for Au@1 and Au@2 are similar to those for the DAT molecules. After exchanging reaction with DT, the FTIR spectra in the high and low frequency regions for DT-exchanged Au@1 and Au@2 are similar to those for the as-synthesized DT-capped gold nanoparticles. The disappearance of the benzene ring breathing bands at $\sim 1600\text{ cm}^{-1}$ and the disappearance of the C(ϕ)-H stretching band at $\sim 3100\text{ cm}^{-1}$ after the exchanging reaction with DT are clear evidence for the replacement of DAT by DT molecules. The changes in these diagnostic regions provided, thus, support for the encapsulation of the as-synthesized Au@1 and Au@2 particles by DAT molecules and the replacement of DATs on the particles by DTs upon the exchange reaction.

It is remarkable that the exchange of DATs on the nanoparticle with the free DTs appeared to be $\sim 100\%$

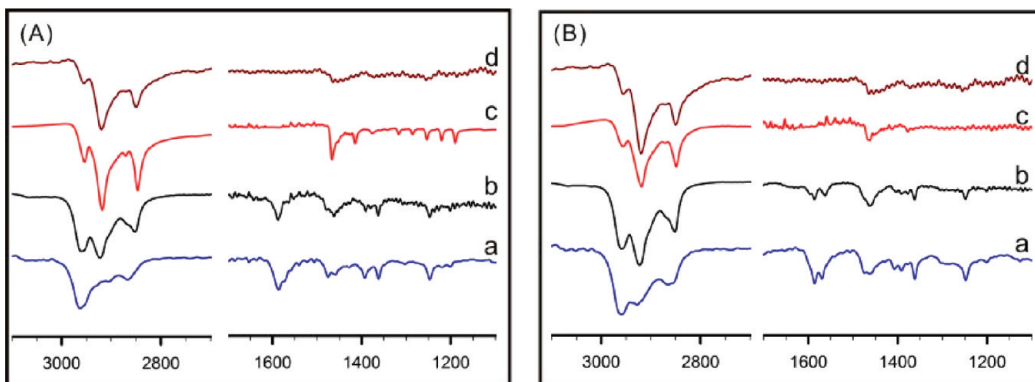


Figure 8. FTIR spectra for DAT (a), DAT-capped gold nanoparticles (b), DAT-capped gold nanoparticle after exchanging with DT (c), and as-synthesized DT-capped gold nanoparticles (synthesized by single-phase method) (d). (A) Au@1; (B) Au@2.

under a 1:0.1 feed ratio of [free thiol ligands]/[capping DATs] according to the FTIR data. In this case, the amount of capping molecules per AuNP was 35 and 50 (average number from Table 2) for **1** and **2**, respectively. In comparison, the degree of exchange was usually 50–70% under a similar feed ratio of [free thiol ligands]/[capping thiol ligands] as demonstrated in previous work¹⁶ (see Supporting Information, Table S1). The high degree of exchange of DATs on nanoparticles with the free MUAs was further proved by FTIR, which showed disappearance of benzene ring breathing bands (1600 and \sim 3100 cm⁻¹) and methyl stretching bands (2955 and 2872 cm⁻¹) and the appearance of the –COOH bands at 1700 cm⁻¹ (see Supporting Information, Figure S3).

Assembly of AuNP–DAT by Molecular Linkers via Exchanging-Cross-Linking Reaction. To further explore the surface reactivity, molecularly mediated assembly of the AuNP–DAT particles via exchanging-cross-linking reaction¹⁷ in solutions were investigated. One example involved the use of 1,9-nonanedithiol (NDT) as a molecular mediator,¹⁸ and the assembly was monitored by the change in the SP band. Figure 9A shows a representative set of UV–vis spectra for the assembly of AuNP–DAT derived from both two-phase and single-phase methods. Upon addition of a solution of NDT (3.3 mM) into the solution of **1**- or **2**-capped gold nanoparticles, a spectral evolution showing the decrease of the 520–525 nm SP band and the increase of absorbance in the longer-wavelength region (650–750 nm) was observed (Figure 9A), demonstrating the interparticle exchanging-cross-linking reactivity. There was no indication of any significant change for the **3**-capped gold nanoparticles upon addition of NDT into the solution under same experimental condition, indicating a lack of the interparticle exchanging-cross-linking reactivity.

The interparticle exchanging-cross-linking reactivity was further assessed in terms of the kinetics of the change

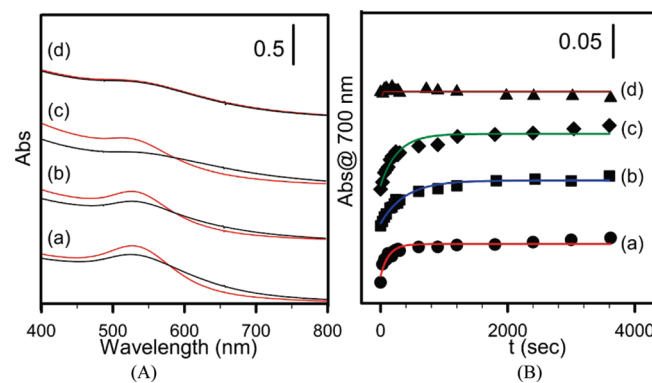


Figure 9. (A) Spectral evolution of SP band in toluene solution containing two-phase synthesized Au@1 (a) and single-phase synthesized Au@1 (b), Au@2 (c), and Au@3 (d) upon addition of NDT ([NDT]/[AuNPs] = 11–26). The reactions were followed for 1 h. (Only the first (red) and the last (black) spectra were shown.) (B) Kinetics for the absorbance at 700 nm for the NDT mediated assemblies of the two-phase synthesized Au@1 (a, $k = 7.7 \times 10^{-3} \text{ s}^{-1}$) and single-phase synthesized Au@1 (b, $k = 3.7 \times 10^{-3} \text{ s}^{-1}$), Au@2 (c, $k = 2.6 \times 10^{-3} \text{ s}^{-1}$), and Au@3 (d). (Lines: first order kinetic fits.)

of the SP band absorbance at 700 nm (Figure 9B). Under the same concentrations, the rate constant for the NDT-mediated assembly of Au@1 ($k = 7.7 \times 10^{-3} \text{ s}^{-1}$) was found to be larger than the assembly of Au@2 ($k = 4.5 \times 10^{-3} \text{ s}^{-1}$) for two-phase synthesized particles. However, the NDT-mediated assembly of Au@1 ($k = 3.7 \times 10^{-3} \text{ s}^{-1}$) was found to be larger than the assembly of Au@2 ($k = 2.6 \times 10^{-3} \text{ s}^{-1}$) for single-phase synthesized particles. The apparent lack of reactivity for the assembly of Au@3 can be explained by the stronger binding of affinity of **3** (*tert*-butylbenzenethiol) to gold particles than **1** and **2**. Moreover, the surface reactivity of larger-sized nanoparticles is stronger than smaller sized particles, which is consistent with previous reports of similar systems.¹³

The interparticle exchanging-cross-linking reactivity was also evidenced by the observation of small aggregates of nanoparticles in the assembly solutions. Figure 10 shows two examples for samples taken from the assembly solution of Au@1 synthesized by two-phase and single-phase methods. Spherical assemblies that are interconnected (A) were observed for the two-phase synthesized Au@1 mediated by NDT. For single-phase synthesized

- (17) (a) Hostetler, M. J.; Templeton, A. C.; Murray, R. W. *Langmuir* **1999**, *15*, 3782. (b) Kassam, A.; Bremner, G.; Clark, B.; Ulibarri, G.; Lennox, R. B. *J. Am. Chem. Soc.* **2006**, *128*, 3476. (c) Montalti, M.; Prodi, L.; Zuccheroni, N.; Baxter, R.; Teobaldi, G.; Zerbetto, F. *Langmuir* **2003**, *19*, 5172.
 (18) Wang, L.; Shi, X.; Kariuki, N. N.; Schadt, M.; Wang, G. R.; Deng, R.; Choi, J.; Luo, J.; Lu, S.; Zhong, C. J. *J. Am. Chem. Soc.* **2007**, *129*, 2161.

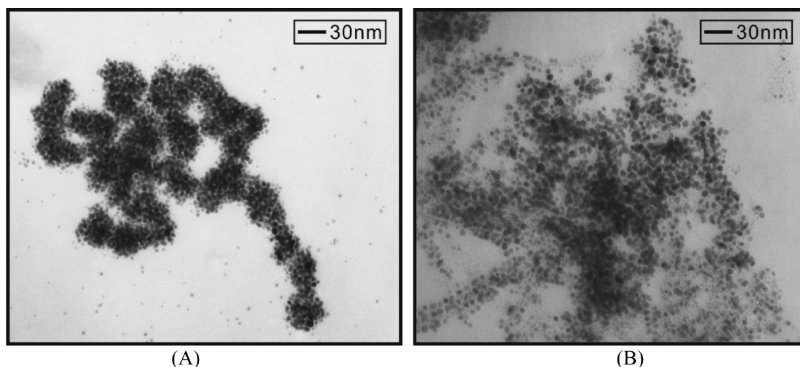


Figure 10. TEM images for samples taken from the solutions of NDT-mediated assemblies of the two-phase (A) and single-phase (B) synthesized $\text{Au}@\mathbf{1}$.

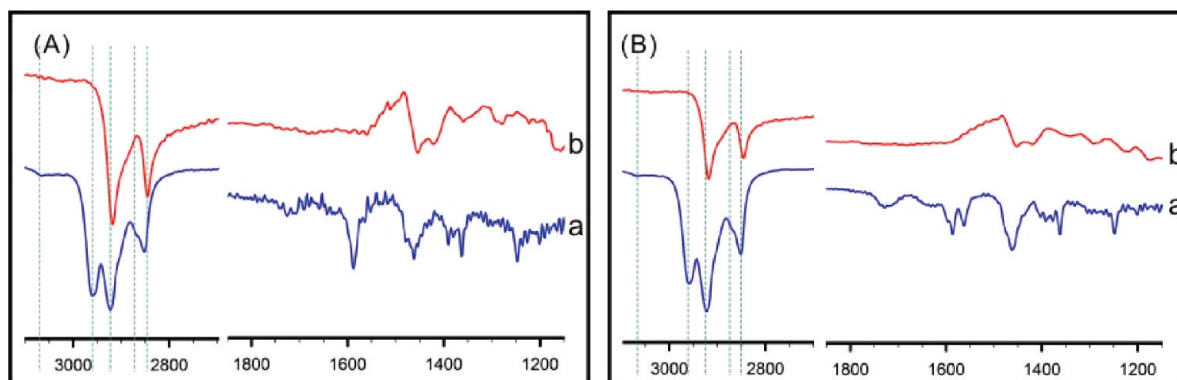


Figure 11. FTIR spectra for DAT-capped gold nanoparticles (synthesized by single-phase method) before (a) and after exchange reaction with NDT (b). (A) $\text{Au}@\mathbf{1}$; (B) $\text{Au}@\mathbf{2}$. Reaction condition: stirring the mixture of DAT-capped gold nanoparticles and NDTs in a toluene solution at room temperature for 24 h, removing the solvent by centrifugation, washing the precipitate copiously with ethanol and hexane, and collecting the product which was dried in the oven for 3 days.

particles $\text{Au}@\mathbf{1}$, the NDT-mediated assemblies were found to form large clusters of nanoparticles (B). The measured interparticle edge-to-edge distance (1.4 nm) for $\text{Au}@\mathbf{1}$ mediated by NDT was found to be close to the length of NDT molecular size.

For the NDT-mediated assemblies, the exchanged product was insoluble in the solution. The replacement of DATs on the nanoparticles by the free NDT molecules was also examined by FTIR characterization. Figure 11 shows a representative set of FTIR spectra for DAT-capped gold nanoparticles before and after the exchange reaction with free NDTs in the solution. The diagnostic features of the spectrum for the DAT-capped gold nanoparticles before the exchange reaction (curve a) include methyl and methylene stretching bands, $\nu_{\text{a,s}}$ (CH_3) (2955 and 2872 cm^{-1}) and $\nu_{\text{a,s}}$ (CH_2) (2920 and 2850 cm^{-1}), in the 2800 – 3000 cm^{-1} region. After the exchange reaction, the absence of the methyl stretching bands (curve b) demonstrates an effective removal of the capping DAT molecules. In comparison with the spectral characteristics for the DAT-capped nanoparticles in the high and low frequency regions, the disappearance of the benzene ring breathing band at $\sim 1600 \text{ cm}^{-1}$ and the $\text{C}(\phi)\text{-H}$ stretching band at $\sim 3100 \text{ cm}^{-1}$ are evident for the $\text{Au}@\mathbf{1}$ and $\text{Au}@\mathbf{2}$ after the exchange reaction with NDTs. In addition, there was no indication of S-H stretching band in the $\sim 2500 \text{ cm}^{-1}$ region, indicative of the conversion of thiol groups to thiolate groups. The changes in these diagnostic

regions, thus, support the replacement of DAT by NDT and the cross-linking of nanoparticles by NDT, which is responsible for the formation of the molecularly mediated assemblies observed from the TEM data. The exchange of the capping DATs with the free NDTs is shown to be $\sim 100\%$ according to the FTIR data. In comparison, under a similar feed ratio ([free thiol ligand]/[capping thiol ligand] (1: 1)), a much smaller value of the exchange degree (15–20%) was reported to be alkanethiol-capped gold nanoparticles¹⁶ (see Supporting Information, Table S1).

In the above FTIR spectra (Figures 8 and 11), it is remarkable that the symmetric and asymmetric C–H stretching bands of methyl groups and the benzene ring breathing bands have completely disappeared for the DAT-capped Au nanoparticles after the exchange reaction, suggesting a high exchange efficiency (nearly 100%) of the DAT molecules on the nanoparticles by NDT molecules, as illustrated in eq 1. In our earlier studies of the place-exchange reaction of different alkanethiolate-capped gold nanoparticles¹⁹ and the exchanging and cross-linking reaction of decanethiolate-capped gold nanoparticles by different molecular linkers (e.g., NDT,

(19) (a) Leibowitz, F. L.; Zheng, W. X.; Maye, M. M.; Zhong, C. J. *Anal. Chem.* **1999**, *71*, 5076. (b) Maye, M. M.; Zheng, W. X.; Leibowitz, F. L.; Ly, N. K.; Zhong, C. J. *Langmuir* **2000**, *16*, 490. (c) Zheng, W. X.; Maye, M. M.; Leibowitz, F. L.; Zhong, C. J. *Anal. Chem.* **2000**, *72*, 2190. (d) Kariuki, N. N.; Han, L.; Ly, N. K.; Peterson, M. J.; Maye, M. M.; Liu, G.; Zhong, C. J. *Langmuir* **2002**, *18*, 8255.

11-mercaptoundecanoic acids, etc.),²⁰ the exchange efficiencies were reported to be much less than 100%, as illustrated in eq 2. Note, however, that these comparisons are only qualitative at this time because the ligand-to-nanoparticle ratios were not exactly identical. While further quantitative comparison is needed, these findings demonstrate the viability of exploiting the umbrella-like structure with a single thiol handle and a spacing-tunable rib for effectively tuning surface reactivity. The easy replacement of the DAT molecules by a ligand having a stronger binding ability to the gold surface than DAT is facilitated by the weak cohesive energy in the capping monolayer of DATs.

Conclusions

The combined weight of these results has demonstrated the feasibility of exploiting the molecular sizes of dendritic arenethiols (DAT) as capping agent for the control of the size and surface reactivity of Au nanoparticles. This type of controllability was achieved by the unique umbrella-like

structure of DATs with a single thiol as the anchorage handle and the rib having an expandable dendritic structure as a spacing-tunable cap. This structure was shown to effectively tune the surface reactivity, as evidenced by the easy replacement of the DAT molecules by a ligand having a stronger binding ability to the gold surface than DAT. One important aspect of this structural character for the size control is the dependence of the binding strength of DATs to gold particles on the “umbrella rib” size, which leads to the capability of controlling the particle sizes. Another important aspect is the combination of the interparticle weak interactions and voids that facilitate the surface reactivity and interparticle assembly by molecular linkers. A detailed delineation of these two aspects with the surface reactivity is part of our further work in fabricating functional assemblies of the nanoparticles for sensing applications.

Acknowledgment. The work was supported by the National Science Foundation (CHE 0848701).

Supporting Information Available: Additional information on the synthesis, TEM, XRD, and DFT data (PDF). This material is available free of charge via the Internet at <http://pubs.acs.org>.

(20) (a) Han, L.; Maye, M. M.; Leibowitz, F. L.; Ly, N. K.; Zhong, C. J. *J. Mater. Chem.* **2001**, *11*, 1258. (b) Han, L.; Luo, J.; Kariuki, N.; Maye, M. M.; Jones, V. W.; Zhong, C. J. *Chem. Mater.* **2003**, *15*, 29.